




Article

The Potential of Shape Memory Alloys in Riveting Applications

Edgar Camacho ¹, Patrícia Freitas Rodrigues ^{2,*} and Francisco Manuel Braz Fernandes ³

¹ ISQ, Department of Research, Development, and Innovation, Instituto de Soldadura e Qualidade, 2740-120 Porto Salvo, Portugal

² ARISE, CEMMPRE, Department of Mechanical Engineering, University of Coimbra, Rua Luís Reis Santos, 3030-788 Coimbra, Portugal

³ CENIMAT/I3N, Department of Materials Science, NOVA School of Science and Technology, 2829-516 Caparica, Portugal

* Correspondence: pf.rodrigues@uc.pt

Abstract: This study explores the use of shape memory alloys, specifically nickel-titanium (NiTi-Ti-rich), in plate joining processes through riveting. Through the shape memory effect (SME), SMAs offer innovative solutions for joining components, mainly in the aeronautical and aerospace fields, indicating their promising applications. This research presents several characterizations, including differential scanning calorimetry, compression dilatometry, X-ray diffraction using synchrotron radiation, and thermomechanical testing, to assess the feasibility and performance of shape memory alloy rivets. In addition, the samples were subjected to recrystallization heat treatment to evaluate their reusability. The results demonstrated that shape memory alloy rivets are effective, achieving a maximum load of 340 N for two joined components. However, their application is optimal for materials with yield strengths lower than the stress-induced SME. Moreover, the process enhances the joined components' hardening and increases the rivet's thermal hysteresis. This research confirms the viability of shape memory alloys for riveting processes, offering a new avenue for advanced joining techniques. The findings provide a foundation for their further development and application in various industries requiring precise and reliable joining methods.

Keywords: shape memory alloys; synchrotron radiation; riveting



Citation: Camacho, E.; Freitas Rodrigues, P.; Braz Fernandes, F.M. The Potential of Shape Memory Alloys in Riveting Applications. *Actuators* **2024**, *13*, 465. <https://doi.org/10.3390/act13110465>

Academic Editors: Hongli Ji and Chao Zhang

Received: 7 October 2024

Revised: 14 November 2024

Accepted: 18 November 2024

Published: 20 November 2024



Copyright: © 2024 by the authors. Licensee MDPI, Basel, Switzerland. This article is an open access article distributed under the terms and conditions of the Creative Commons Attribution (CC BY) license (<https://creativecommons.org/licenses/by/4.0/>).

1. Introduction

Riveting has been a cornerstone of mechanical joining since the early days of metallurgy, playing a crucial role in industries like aeronautics and aerospace. It involves the plastic deformation of a cylindrical pin, usually crafted from the same material as the components being joined. This process secures structural frameworks by forming a permanent mechanical bond between panels and other critical components. Traditional riveting techniques, however, come with inherent limitations, such as a finite service life, potential loosening of joints due to vibration, and the need for their periodic maintenance and replacement to preserve structural integrity. To address these challenges, exploring innovative materials, such as shape memory alloys (SMAs), has gained considerable attention [1–4].

Shape memory alloys, specifically nickel-titanium (NiTi) alloys, exhibit unique properties that offer the potential to overcome the drawbacks of traditional riveting. First discovered by [1], NiTi alloys are distinguished by their ability to undergo a reversible phase transformation in the solid state. This transformation occurs between the martensitic (low-temperature) and austenitic (high-temperature) phases, making NiTi highly effective in applications where deformation recovery and mechanical performance are critical. NiTi's phase transformation is diffusionless, typically occurring at an equiatomic ratio of approximately 50% nickel and 50% titanium. These transformations enable two fundamental mechanisms, the shape memory effect (SME) and superelasticity (SE), both of which can be harnessed to enhance the functionality of riveted joints [5–9].

The SME is thermally induced, where deformation in the martensitic state can be fully recovered upon heating beyond the transformation temperature. At the same time, SE occurs through stress-induced phase changes above the austenitic finish temperature (A_f), allowing full recovery upon unloading [10–13]. Due to these properties, NiTi alloys are particularly suited for applications requiring high fatigue resistance and mechanical stability, such as those in the aerospace sector. In riveting, the SME can be exploited by heating the NiTi rivet during installation, allowing it to contract axially and expand radially, thus filling gaps and providing enhanced tension between the rivet and the joined plates. This feature improves both joint stability and longevity by compensating for the typical loss of radial tension experienced in traditional riveting [7]. Recent studies suggest that a higher titanium content raises transformation temperatures, whereas a higher nickel content lowers them, underscoring the need to tailor alloy composition to specific operational conditions, particularly in aerospace applications where rivets must remain in the austenitic phase to ensure structural integrity [12,13].

The martensitic transformation in NiTi alloys is also characterized by specific transformation temperatures, denoted as M_s (martensitic start), M_f (martensitic finish), R_s (R-phase start), R_f (R-phase finish), A_s (austenitic start), and A_f (austenitic finish). These temperatures are critical in determining the material's behavior during mechanical loading and highly depend on the alloy composition [14,15]. Alloys with a higher titanium content generally exhibit higher transformation temperatures, while those richer in nickel tend to have lower transformation points. This sensitivity to composition makes it essential to tailor the NiTi alloy for specific operational conditions, especially in high-demand environments such as aerospace, where the rivets must remain in the austenitic phase throughout service to maintain structural integrity [16–18].

Crystallographic anisotropy in NiTi alloys further influences their mechanical behavior. Studies by Gall et al. and Liu et al. demonstrated that the mechanical properties of NiTi single crystals differ significantly under tension and compression, depending on the crystallographic orientation. This anisotropy affects deformation mechanisms such as martensitic twinning or variant reorientation, which is essential for understanding how NiTi behaves under mechanical stress during the riveting process [19].

Despite the potential advantages, traditional riveting methods remain limited by certain mechanical shortcomings, such as decreasing radial tension after installation, which can lead to joint loosening and reduced vibration resistance. However, using SMAs, particularly NiTi alloys, in riveting offers a promising alternative. NiTi rivets can actively adapt to fill gaps and increase the joint's tensile strength and fatigue resistance by exploiting the SME during the riveting process. This adaptive behavior has been explored in patents and studies, with companies like Boeing suggesting that NiTi rivets could revolutionize aerospace joining techniques by reducing maintenance requirements and improving overall joint performance [20].

One key consideration in applying NiTi SMAs to riveting is the operational temperature range of the components being joined. The transformation temperatures of the NiTi rivets must remain below the service environment's minimum temperature to avoid unintended martensitic transformation during operation, which could compromise joint stability. Additionally, thermal hysteresis, which refers to the difference between the transformation and reversion temperatures, must be carefully managed to ensure the rivets maintain consistent performance throughout their service life. To address these considerations and validate the feasibility of NiTi alloys in riveting methods, a proof-of-concept was performed, demonstrating the potential of using SME-based rivets to improve joint strength and stability [21–24].

Recent advances in shape memory alloy (SMA) technology have highlighted the importance of microstructural stability and phase transformation mechanisms in enhancing mechanical performance, particularly for high-stress applications like riveting. Studies indicate that fine-tuning the microstructure of nickel-titanium (NiTi) alloys, through techniques such as thermomechanical processing and elemental adjustments, can significantly

improve their fatigue resistance and superelastic properties, making them suitable for environments with high mechanical demands [25]. Additionally, innovations in the compositional design of NiTi-based SMAs underscore the potential of these alloys to sustain repeated phase transformations with minimal degradation, thereby increasing their reliability and lifespan under cyclic loading conditions common in aerospace applications [26]. These findings strengthen the rationale for exploring SMAs in riveting, as enhanced phase stability and superelasticity directly address limitations seen in traditional rivet materials, such as susceptibility to loosening and reduced vibration resistance.

While the potential of SMAs in various engineering applications has been well-documented, research specifically focused on the use of NiTi alloys in riveting remains limited. One notable gap is the lack of comprehensive experimental studies that directly compare the performance of NiTi rivets to traditional materials, such as aluminum and steel, in terms of long-term fatigue resistance and joint integrity. Furthermore, there is a need for deeper exploration of how the shape memory effect in NiTi rivets can mitigate the loosening and gap formation issues commonly observed in conventional riveting methods. The literature also requires studies that examine the reusability and repairability of NiTi rivets after heat treatment, especially in high-temperature environments, which is crucial for aerospace applications [27,28].

Given these gaps, this study seeks to (i) optimize the actuation force of NiTi SMA rivets for enhanced joint performance, and (ii) analyze the effects of heat treatment and recrystallization on their reusability, particularly in advanced aeronautical and aerospace applications. By exploring these areas, this research aims to provide novel insights into how NiTi alloys can be effectively utilized to improve the durability, strength, and efficiency of riveted joints in high-performance environments.

2. Materials and Methods

2.1. Materials

The materials used in this study included a Ti-rich NiTi alloy sourced from Memry GmbH, (Weil a. Rhein, Germany) H-alloy, supplied in cold-worked rod form with a diameter of 9.525 mm and an oxide layer. Recrystallization heat treatments were carried out at 500 °C for 30 min, followed by water quenching, using a Termolab MLM furnace (Águeda, Portugal). This was performed to relieve internal stresses and enhance the shape memory effect (SME) performance of the rivets. Aluminum plates were used for joint tests, serving as representative materials for evaluating the performance of SME rivets in practical applications.

2.2. Proof of Concept

For the proof-of-concept tests (Figure 1a), 3 mm thick aluminum plates with a width of 30 mm were used, although specific details about the alloy composition were not provided. Electro-discharge machining (EDM) was employed to prepare both the NiTi and aluminum samples (Figure 1b). The NiTi rivets were inserted into the aluminum plates, and forced heating with an output temperature of 500 °C triggered the SME activation. The surface temperature of the proof-of-concept jig was measured at 150 °C using a thermocouple (Figure 1c).

2.3. Characterization Techniques

2.3.1. Differential Scanning Calorimetry

The thermal behavior of the samples was analyzed using a NETZSCH DSC 204 F1 Phoenix (NETZSCH-Gerätebau GmbH, Wittelsbacher straÙe, Germany). The heating and cooling rates were set at 10 °C/min, with a thermal stabilization plateau of 5 min. The thermal cycle followed the profile: room temperature/150 °C/−150 °C/150 °C. A protective nitrogen atmosphere was maintained with a gas flow rate of 20 mL/min, while liquid nitrogen was supplied at 2 mL/min. These parameters allowed for the precise determination of the transformation temperatures.

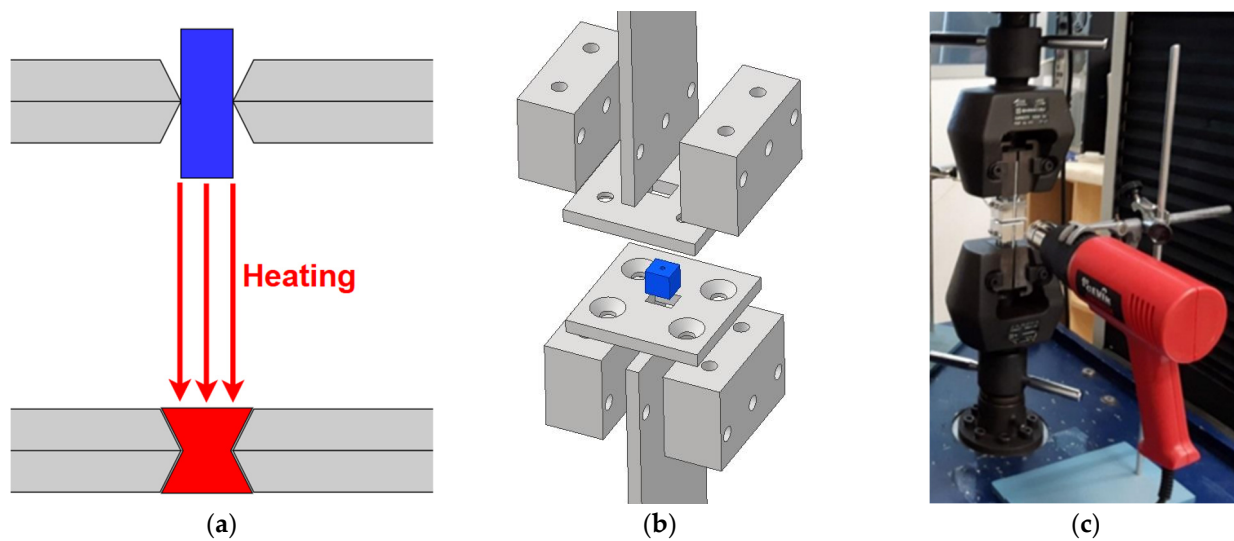


Figure 1. Proof of concept scheme—(a) SME concept rivet; (b) exploded view drawing of the prototype; and (c) test assembly method.

2.3.2. Thermo-Mechanical Tests

Linseis model TMA PT1600 (Linseis Messgeraete GmbH, Vielitzerstr, Germany) was used for dilatometry tests. This equipment provided detailed measurements of thermal expansion and contraction behavior in the NiTi samples during thermal cycles. The dilatometry results were crucial for understanding the thermal responses under varying stress and temperature conditions.

2.3.3. Mechanical Tests

Mechanical properties were evaluated using the AUTOGRAPH SHIMADZU (Duisburg, F.R. Germany) model AG500Kng with a load cell rated for a maximum load of 50 kN. This system applied a load to the samples under controlled conditions to determine their tensile strength, SME performance, and response to thermomechanical deformation.

2.3.4. Synchrotron Radiation X-Ray Diffraction

For crystallographic analysis, SR-XRD was performed at beamline P07 High-Energy Materials Science (HEMS) of Petra III/DESY. The measurements were carried out in transmission mode on rod-shaped samples (5 mm diameter, 10 mm height) at room temperature. A wavelength of 0.1426 Å (103.3 keV) was used, with the PERKIN ELMER XRD 1621 two-dimensional detector placed 2.00 m from the sample. Raw 2D images were processed using Fit2D software (Version 18 (beta)) to calculate integrated XRD patterns, specifically across azimuthal angles from 355° to 5°, as these angles were the most perpendicular to the direction of deformation during the experiment. The diffraction peaks were identified using the ICDD database.

3. Results

3.1. Mechanical Behavior

The stress-strain results highlight the material's anisotropic mechanical behavior, showing distinct differences between its axial and radial directions (Figure 2). The radial direction exhibits a sharper increase in stress, reaching a maximum of approximately 1200 MPa at 13% strain, while the axial direction peaks at around 800 MPa at the same strain. This suggests that the material is more resistant to deformation under radial stress. Stress points σ_{ts} (twinning start) and σ_{tf} (twinning finish) indicate that there was a twinning reorientation, after which the material undergoes plastic deformation. These properties indicate that the material's anisotropy can benefit applications where strength varies by direction, with the radial orientation providing a superior performance. The curves' non-

linear behavior, characteristic of materials like Shape Memory Alloys (SMAs), underscores the role of the shape memory effect (SME) and superelasticity in enabling the material to recover its shape after deformation [7,29].

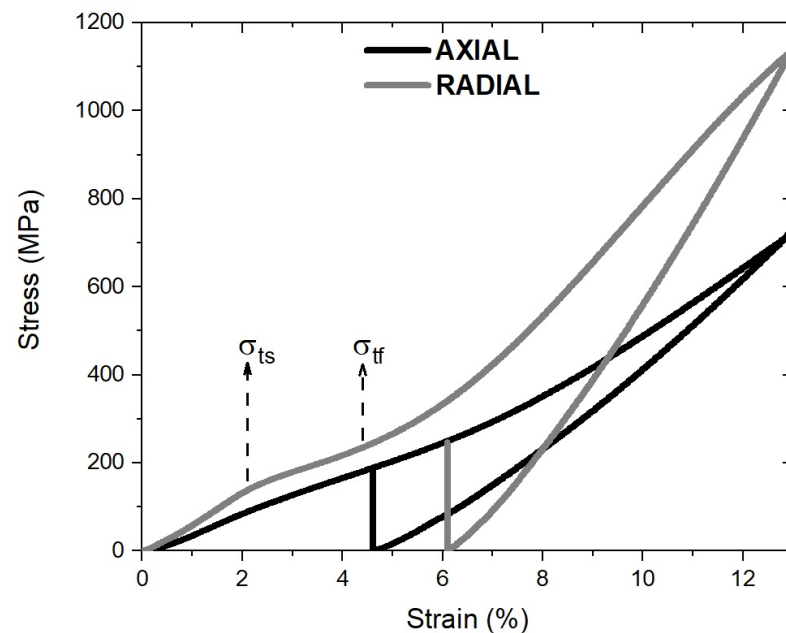


Figure 2. Stress-strain, axial and radial mechanical behavior.

The mechanical tests also provide key insights into the strength and deformation behavior of the NiTi alloy, which is crucial for its use in mechanical joints. Compressive testing of up to a 16.7% strain showed a significant % elastic recovery of 7.8%. When heated above the austenite start (A_s) temperature, the SME was triggered, reaching a maximum stress of 246 MPa. This highlights the alloy's ability to return to its original shape, an essential property for applications requiring mechanical durability and precise actuation. The SME allows the material to “remember” its pre-deformed state, enabling enhanced performance in scenarios that demand shape recovery and superelasticity.

In comparison, the aluminum alloy used for prototype joints exhibited different mechanical properties under compressive testing, with a yield strength of around 115 MPa. It demonstrated significant plasticity, allowing for considerable deformation before failure, making it well-suited for joint applications where controlled deformation is required for bonding. The combination of NiTi and aluminum is advantageous because of their complementary behaviors [30].

Using NiTi as a rivet and aluminum as the joined material offers a promising solution for mechanical joints. The aluminum undergoes localized plastic deformation, which can induce stress hardening at the interface, enhancing joint strength and stability. Stress hardening increases the aluminum's resistance to further deformation, reinforcing the mechanical interlock between the rivet and the joined material. This, along with the superelasticity and SME of NiTi, ensures a secure and durable joint capable of withstanding long-term mechanical stress [2,31].

NiTi's superelastic properties allow it to accommodate stress through reversible deformations. Combined with the stress-hardened aluminum, the NiTi rivet maintains a stable, leak-proof bond, even under dynamic loads or environmental variations (Figure 3). This property makes the joint resistant to mechanical fatigue and loosening caused by vibrations or thermal expansion, which is ideal for high-performance applications like those in the aerospace and automotive industries. Moreover, the SME in the NiTi rivet allows the joint to adapt to changing conditions, adding an extra layer of stability and ensuring its structural integrity over time.

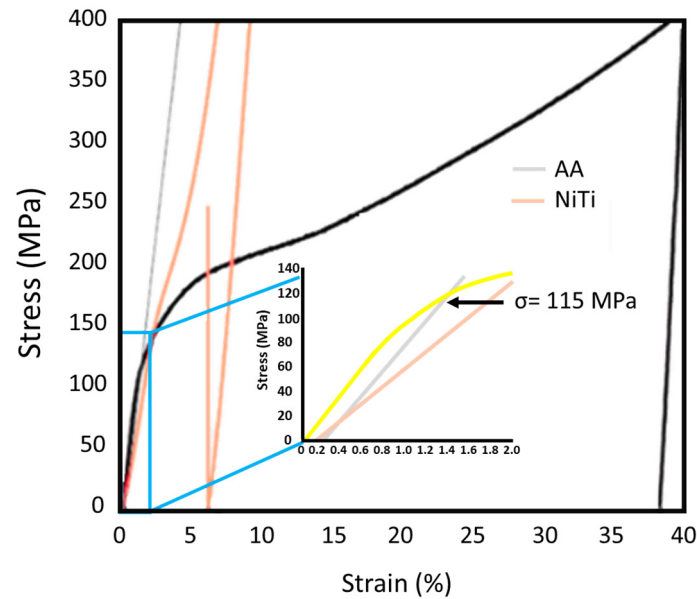


Figure 3. Comparison of stress-strain curves between aluminum plates and NiTi alloy.

The presented results highlight the complex relationship between stress, strain, and temperature in the material, exhibiting behavior typical of shape memory alloys (SMAs) (Figure 4). At room temperature, the material demonstrates elastic deformation until reaching the stress threshold (σ_s), where phase transformation begins. As strain increases, the tension rises non-linearly, indicating the occurrence of martensitic transformation, and reaches a maximum stress (σ_f) of around 1600 MPa before failure. Figure 4 also displays that, with increasing temperature, the material experiences a significant recovery of residual strain, confirming the activation of the shape memory effect (SME). The transformation strain (ϵ_{Tr}) and residual strain ($\epsilon_{residual}$) are observed at different stages of loading and heating, emphasizing the material's ability to recover its shape when subjected to thermal cycling. This temperature-dependent recovery behavior, along with the superelasticity indicated by the high-stress values, makes SMAs highly suitable for applications that require cyclic loading and recovery, such as aerospace and mechanical actuators. The results underscore the material's capacity to resist significant mechanical stress while maintaining its functional integrity across varying temperature ranges.

3.2. Thermal and Thermo-Mechanical Behavior

The Differential Scanning Calorimetry (DSC) analysis of the Ti-rich NiTi alloy, shown in Figure 5, illustrates the thermal behavior and phase transformation temperatures during the first and second heating and cooling cycles, coupled with dilatometry results. The transformation temperatures are clearly indicated, with the first heating cycle showing the martensite finish (M_f) at 36 °C, the martensite start (M_s) at 55.3 °C, the austenite start (A_{s1}) at 123.3 °C, and the austenite finish (A_{f1}) at 137.7 °C. During the second heating, the austenite start (A_{s2}) occurred at 92.1 °C and the austenite finish (A_{f2}) at 105.8 °C.

A noticeable shift between the first and second thermal cycles is observed, primarily due to the reorientation of martensitic twins during mechanical deformation, which requires additional heat during the second cycle for the shape memory effect (SME) to occur. The DSC curves highlight how mechanical deformation alters the thermal response, as evidenced by the increased A_s temperature in the first heating cycle. Once the A_f temperature is surpassed, the full recovery of the material's original shape occurs. The differences in A_s and A_f temperatures between the cycles indicate a shift in the material's transformation kinetics, making it well-suited for applications where actuation and recovery are critical.

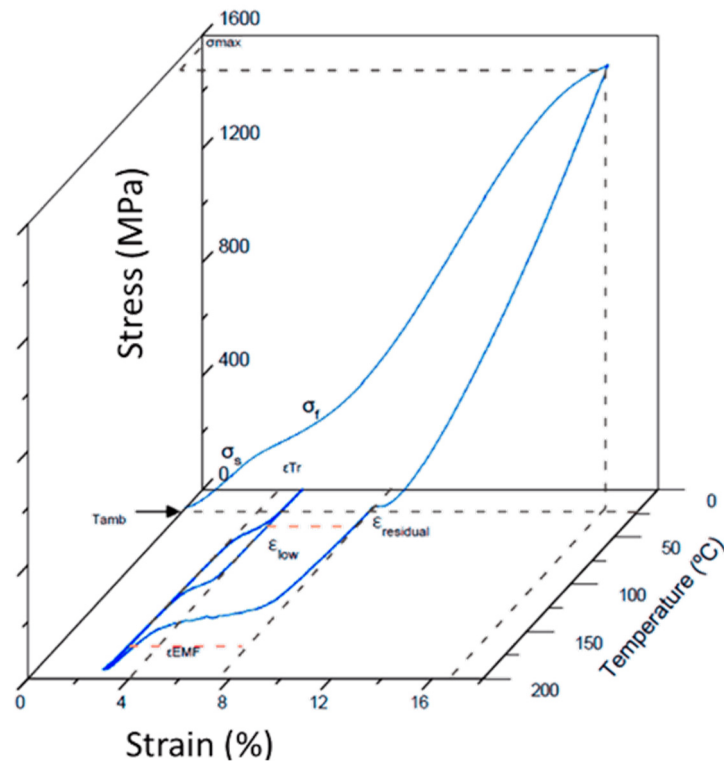


Figure 4. Stress-strain-temperature curves of shape memory effect.

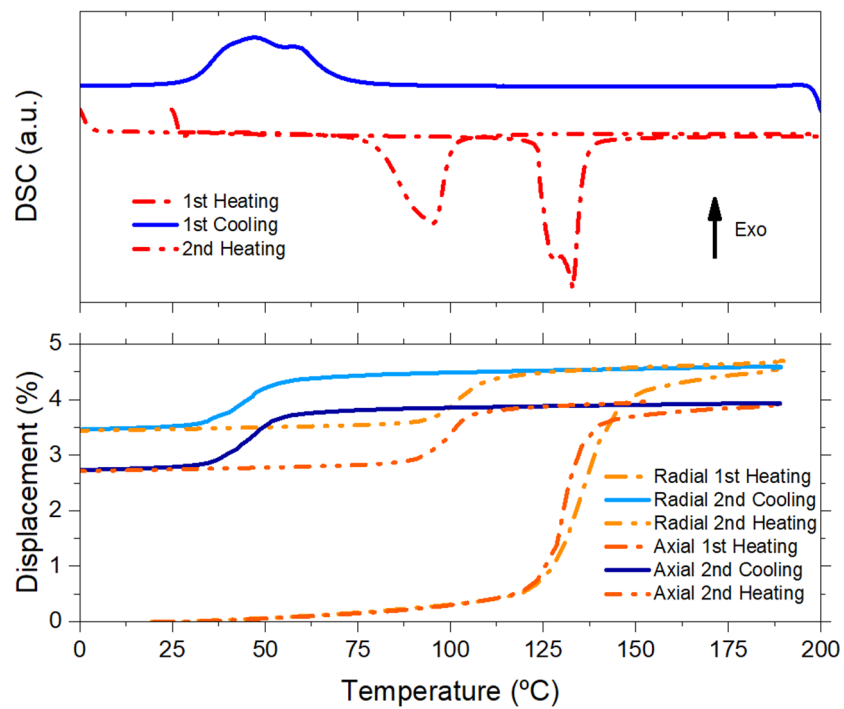


Figure 5. DSC and dilatometry curves of NiTi alloy.

The dilatometry curves further support these findings by showing significant differences in strain recovery during the first and second heating cycles for both the radial and axial directions. During the first heating, both the axial and radial directions exhibit a sharp increase in length around 125 °C, correlating with the SME activation and the material’s ability to revert to its pre-deformed state. A maximum strain recovery of approximately 4.6% was achieved, confirming the material’s high actuation potential. This actuation force,

with peak stresses reaching 246 MPa, underscores the alloy's capability for applications requiring robust and repeatable recovery, such as in rivet systems.

Additionally, the second heating cycle demonstrates a more stable and less pronounced phase transformation, indicating that after the initial deformation and recovery, the material experiences less residual strain and more predictable behavior. This behavior highlights the material's potential for long-term reliability in thermal cycling environments, making it suitable for applications like SME-based rivets, where durability and repeated actuation are crucial.

3.3. Synchrotron Radiation X-Ray Diffraction Results

The in-situ synchrotron radiation X-ray diffraction (SR-XRD) analysis provides crucial insights into the crystallographic evolution of the NiTi alloy during different phases of deformation and thermal recovery (Figure 6). The study compares four stages: the initial state, maximum deformation, post-deformation, and post-thermal recovery. These diffraction patterns reveal significant structural changes that inform the material's response under mechanical stress and heating, particularly related to the shape memory effect (SME) and superelasticity.

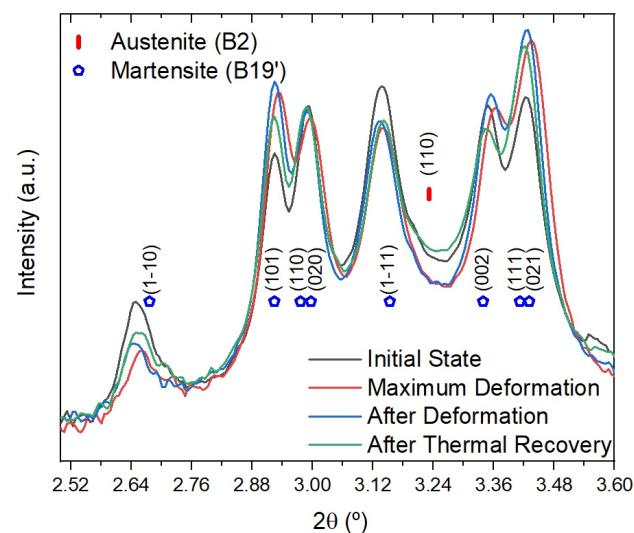


Figure 6. SR-XRD diffractograms—the initial state, maximum deformation, post-deformation, and post-thermal recovery.

In comparing the initial state to the maximum deformation, there is a notable decrease in the peak intensity for the following B19 crystallographic planes (1 $\bar{1}$ 0), (0 2 0), and (1 $\bar{1}$ 1). This intensity drop suggests that detwinning occurred during deformation, where some twins were realigned or removed to accommodate the strain, reinforcing certain planes such as (1 0 1) and (0 2 1). Interestingly, the plane (0 0 2) remained unchanged during deformation, indicating stability in that particular orientation despite the mechanical stress.

Between maximum deformation and post-deformation, the material shows signs of elastic recovery. This recovery is evidenced by slight translations in the 2θ peaks and small increases in intensity, signaling that strain-induced twin rearrangement had occurred. The observed changes in the diffraction peaks support the material's superelastic nature, with its structure adapting and partially recovering after removing the mechanical load.

Finally, in the transition from post-deformation to post-thermal recovery, a slight increase in intensity for the plane (1 $\bar{1}$ 0) and a small shift in peak position reflect stress relief due to thermal cycling. The SME plays a crucial role in this stage, as some of the crystallographic planes that were initially reinforced during deformation (such as (1 0 1), (0 0 2), and (1 1 1)) experience a reduction in intensity, indicating that the twins, which contributed to the material's ability to withstand stress, are reoriented or detwinned.

during recovery (Figure 7). Conversely, no significant changes were observed in the planes (0 2 0) and (1 − 1 1), highlighting that these planes are less responsive to deformation and recovery cycles.

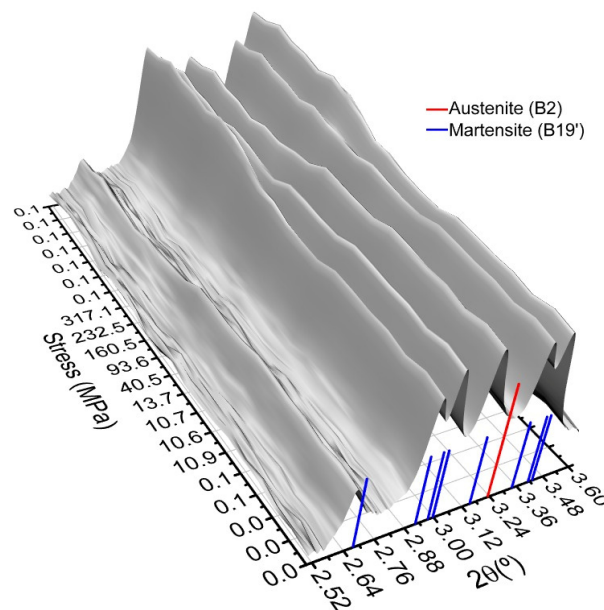


Figure 7. SR-XRD diffractograms of the transition between maximum deformation and post-deformation.

3.4. Rivet Application Testing

The rivet application tests confirmed the effectiveness of using Ti-rich NiTi alloys in shape memory effect (SME)-based rivets for joining applications. The electro-eroded rivet was successfully inserted into aluminum plates, and the joint remained intact under an applied separation force of 340 N. This strong bond was achieved through SME actuation, triggered by heating the rivet to 500 °C, with a corresponding surface temperature of 150 °C on the aluminum. The combination of SME activation and the wedged design of the aluminum plates provided significant mechanical strength, enabling the joint to withstand high stress without failure.

The results demonstrate that NiTi alloy SME rivets can form robust and reliable joints, provided that the service temperature stays above the austenite finish temperature (A_f), ensuring consistent actuation and bonding strength (Figure 8). The performance of the SME rivets under mechanical loading further highlights their potential for use in high-performance applications, where durability and thermal activation are critical. The experimental evidence suggests that Ti-rich NiTi SME rivets are highly suitable for advanced joining processes in industries such as aerospace and automotive engineering, where precise and long-lasting mechanical connections are required.

This study has demonstrated the potential of shape memory alloys (SMAs), particularly NiTi alloys, for riveting applications, highlighting their adaptability, mechanical strength, and durability in high-demand environments such as the aerospace sector. However, for effective practical implementation, future research should explore advanced coating approaches that could further enhance the structural performance and corrosion resistance of these rivets. For instance, the development of high-performance SMA coatings specifically designed for structural aerospace applications could significantly improve component longevity [32]. Additionally, ZrO₂-CaF₂ composite coatings applied via low-pressure plasma spraying have shown potential for improved high-temperature tribological properties, which could benefit NiTi rivets operating under extreme thermal conditions [33]. These advances could lead to more corrosion-resistant rivets, extending their service life and reducing their maintenance needs in aerospace structures. Future research, integrating advanced coatings with SMAs in rivets, could open up new possibilities for high-performance

applications, combining the mechanical adaptability of NiTi alloys with superior protection against wear and corrosion.

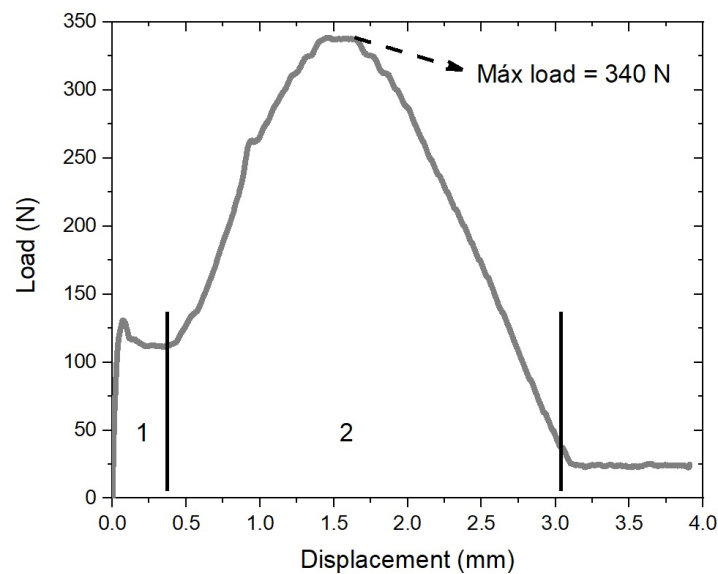


Figure 8. Shape memory effect: deformation with heating recovery.

4. Conclusions

This study aimed to assess the viability of using a Ti-rich NiTi alloy to shape memory effect (SME) rivets in joining processes, and the results provided important insights into their potential for practical applications. The Ti-rich NiTi alloy exhibited well-defined thermal hysteresis, excellent strain recovery, and high actuation stress, positioning it as a promising candidate for SME rivet applications. Mechanical characterization revealed a maximum actuation stress of 246 MPa for the NiTi alloy, with the aluminum alloy used as the joined component showing a yield strength of approximately 115 MPa. This combination suggests that the NiTi alloy could effectively function as a rivet, with the aluminum serving as a compatible material in the joint. Thermomechanical testing demonstrated higher austenite start (A_s) and austenite finish (A_f) temperatures during the first thermal cycle compared to subsequent cycles, with a free recovery of 4.6% through SME, further supporting the alloy's suitability for actuation-based applications. Synchrotron radiation X-ray diffraction (SR-XRD) analysis revealed that specific crystallographic planes in the NiTi alloy undergo detwinning during mechanical deformation and recovery during thermal cycling, with certain planes showing greater strain sensitivity. Prototype SME rivets were successfully tested by joining aluminum plates, maintaining their joint integrity until a force of 340 N was applied, demonstrating the effectiveness of SME-based rivets in mechanical connections. These findings confirm the feasibility of applying SME to rivets, particularly using Ti-rich NiTi alloys, which exhibit excellent mechanical and thermal performance, making them strong candidates for rivet applications across various industries. Future research should aim to optimize the thermal and mechanical properties of SME rivet materials and investigate joining materials that complement the NiTi alloy's SME behavior. Additionally, further exploration of crystallographic textures and thermal recovery under constant stress will be essential for enhancing the performance of SME rivets, particularly in applications requiring lightweight materials and strong, durable mechanical connections.

Author Contributions: Conceptualization, E.C. and F.M.B.F.; methodology, E.C. and P.F.R.; validation, P.F.R. and F.M.B.F.; formal analysis, E.C.; investigation, E.C. and P.F.R.; resources, F.M.B.F.; data curation, E.C. and P.F.R.; writing—original draft preparation, E.C.; writing—review and editing, P.F.R. and F.M.B.F.; visualization, E.C.; supervision, F.M.B.F.; funding acquisition, F.M.B.F. All authors have read and agreed to the published version of the manuscript.

Funding: This research was supported by national funds through FCT—Fundação para a Ciência e a Tecnologia, under projects UIDB/00285/2020 and LA/P/0112/2020. FMBF acknowledges funding by national funds from FCT—Fundação para a Ciência e a Tecnologia, LA/P/0037/2020, UIDP/50025/2020, and UIDB/50025/2020 of the Associate Laboratory Institute of Nanostructures, Nanomodelling and Nanofabrication—i3N. Parts of this research were carried out at beamline P-07 at DESY, a member of the Helmholtz Association (HGF). The research leading to this result has been supported by the project CALIPSOplus under the Grant Agreement 730872 from the EU Framework Programme for Research and Innovation HORIZON 2020.

Data Availability Statement: Data are contained within the article.

Conflicts of Interest: The authors declare no conflicts of interest.

References

1. Buehler, W.J.; Gilfrich, J.V.; Wiley, R.C. Effect of Low-Temperature Phase Changes on the Mechanical Properties of Alloys near Composition TiNi. *J. Appl. Phys.* **1963**, *34*, 1475–1477. [CrossRef]
2. Koh, J.S. Design of Shape Memory Alloy Coil Spring Actuator for Improving Performance in Cyclic Actuation. *Materials* **2018**, *11*, 2324. [CrossRef] [PubMed]
3. Mabe, J.H.; Calkins, F.T.; Bushnell, G.S.; Bieniawski, S.R. Aircraft Systems with Shape Memory Alloy (SMA) Actuators, and Associated Methods. Patent no. US 7,878,459 B2, 2011. Available online: <https://patents.google.com/patent/US7878459B2/en> (accessed on 1 June 2022).
4. Abdullah, E.J.; Gaikwad, P.S.; Azid, N.; Majid, D.L.A.; Rafie, A.S.M. Temperature and strain feedback control for shape memory alloy actuated composite plate. *Sens. Actuators A Phys.* **2018**, *283*, 134–140. [CrossRef]
5. Yuan, H.; Fauroux, J.C.; Chapelle, F.; Balandraud, X. A review of rotary actuators based on shape memory alloys. *J. Intell. Mater. Syst. Struct.* **2017**, *28*, 1863–1885. [CrossRef]
6. Patra, N.; Geetha, S.R.; Harish, C.; Chouhan, N.; Singh, V.; Palani, I.A. Compositional influence of CuAlMn SMA coated optical fiber towards sensing low temperature. *Sens. Actuators A Phys.* **2024**, *366*, 114997. [CrossRef]
7. Patel, S.K.; Swain, B.; Roshan, R.; Sahu, N.K.; Behera, A. A brief review of shape memory effects and fabrication processes of NiTi shape memory alloys. *Mater. Today Proc.* **2020**, *33*, 5552–5556. [CrossRef]
8. Sadashiva, M.; Sheikh, M.Y.; Khan, N.; Kurbet, R.; Gowda, T.M.D. A Review on Application of Shape Memory Alloys. *Int. J. Recent Technol. Eng. (IJRTE)* **2021**, *9*, 111–120. [CrossRef]
9. Braz Fernandes, F.M.; Camacho, E.; Rodrigues, P.F.; Inácio, P.; Santos, T.G.; Schell, N. In Situ Structural Characterization of Functionally Graded Ni–Ti Shape Memory Alloy During Tensile Loading. *Shape Mem. Superelasticity* **2019**, *5*, 457–467. [CrossRef]
10. Suzuki, Y. Fabrication of shape memory alloys. In *Shape Memory Materials*, 1st ed.; Otsuka, K., Wayman, C.M., Eds.; Cambridge University Press: New York, NY, USA, 1998; pp. 133–148.
11. Saburi, T. Ti–Ni Shape memory Alloys. In *Shape Memory Materials*, 1st ed.; Otsuka, K., Wayman, C.M., Eds.; Cambridge University Press: New York, NY, USA, 1998; pp. 49–96.
12. Gangil, N.; Siddiquee, A.N.; Maheshwari, S. Towards applications, processing and advancements in shape memory alloy and its composites. *J. Manuf. Process* **2020**, *59*, 205–222. [CrossRef]
13. Wang, Z.; Luo, J.; Kuang, W.; Jin, M.; Liu, G.; Jin, X.; Shen, Y. Strain Rate Effect on the Thermomechanical Behavior of NiTi Shape Memory Alloys: A Literature Review. *Metals* **2022**, *13*, 58. [CrossRef]
14. Braga, R.; Rodrigues, P.F.; Cordeiro, H.; Carreira, P.; Vieira, M.T. The Study of New NiTi Actuators to Reinforce the Wing Movement of Aircraft Systems. *Materials* **2022**, *15*, 4787. [CrossRef] [PubMed]
15. Lima, P.C.; Rodrigues, P.F.; Ramos, A.S.; da Costa, J.D.M.; Fernandes, F.M.B.; Vieira, M.T. Experimental Analysis of NiTi Alloy during Strain-Controlled Low-Cycle Fatigue. *Materials* **2021**, *14*, 4455. [CrossRef] [PubMed]
16. Behrooz, M.; Gordaninejad, F. Three-dimensional study of a one-way, flexible magnetorheological elastomer-based micro fluid transport system. *Smart Mater. Struct.* **2016**, *25*, 095012. [CrossRef]
17. Velmurugan, C.; Senthilkumar, V.; Dinesh, S.; Arulkirubakaran, D. Review on phase transformation behavior of NiTi shape memory alloys. *Mater. Today Proc.* **2018**, *5*, 14597–14606. [CrossRef]
18. Lu, Y.; Zhang, R.; Xu, Y.; Wang, L.; Yue, H. Resistance Characteristics of SMA Actuator Based on the Variable Speed Phase Transformation Constitutive Model. *Materials* **2020**, *13*, 1479. [CrossRef]
19. Mall, S.; Coleman, J.M. Monotonic and fatigue loading behavior of quasi-isotropic graphite/epoxy laminate embedded with piezoelectric sensor. *Smart Mater. Struct.* **1998**, *7*, 822–832. [CrossRef]
20. Dzugbewu, T.C.; de Beer, D.J. Additive manufacturing of NiTi shape memory alloy and its industrial applications. *Heliyon* **2024**, *10*, e23369. [CrossRef]
21. Chiang, T.H.; Thatcher, D.N. Chiang, Forming Apparatus Employing a Shape Memory Alloy Die. U.S. Patent No. 4,797,085, 10 January 1989.
22. Shimoga, G.; Kim, T.H.; Kim, S.Y. An Intermetallic NiTi-Based Shape Memory Coil Spring for Actuator Technologies. *Metals* **2021**, *11*, 1212. [CrossRef]

23. Garudapalli, A.; Bhardwaj, A.; Oswal, K.; Mathur, D.; Gupta, A.K. Microstructural, Mechanical, and Superelastic Behavior of Thermo-Mechanically Processed Nitinol Alloy. *Shape Mem. Superelasticity* **2021**, *7*, 503–514. [[CrossRef](#)]
24. Hunek, M.; Pliva, Z. *Design and Optimisation of NiTi Pressure Gauge*; Institute of Electrical and Electronics Engineers (IEEE): Piscataway, NJ, USA, 2017; pp. 1–3. [[CrossRef](#)]
25. Lu, H.Z.; Liu, L.H.; Yang, C.; Luo, X.; Song, C.H.; Wang, Z.; Wang, J.; Su, Y.D.; Ding, Y.F.; Zhang, L.C.; et al. Simultaneous enhancement of mechanical and shape memory properties by heat-treatment homogenization of Ti₂Ni precipitates in TiNi shape memory alloy fabricated by selective laser melting. *J. Mater. Sci. Technol.* **2022**, *101*, 205–216. [[CrossRef](#)]
26. Yang, C.; Huang, Z.Y.; Chen, T.; Lu, H.Z.; Ma, H.W.; Li, H.Z.; Yan, A.; Li, P.X.; Hosoda, H.; Cai, W.S. Large recoverable strains with high recovery rates via cooperative regulation of texture and precipitation in additive manufactured NiTi alloy. *Scr. Mater.* **2024**, *248*, 116122. [[CrossRef](#)]
27. Otsuka, K.; Ren, X. Recent developments in the research of shape memory alloys. *Intermetallics* **1999**, *7*, 511–528. [[CrossRef](#)]
28. Luo, J.; Xu, G.; Zhang, Q.; Li, Y.; He, J. Deformation mechanisms of a NiTi alloy under high cycle fatigue. *J. Mater. Res. Technol.* **2022**, *21*, 2693–2703. [[CrossRef](#)]
29. Otsuka, K.; Wayman, C.M. Mechanism of shape memory effect and superelasticity. In *Shape Memory Materials, First*; Cambridge University Press: New York, NY, USA, 1998.
30. Fernandes, F.M.B.; Camacho, E.; Rodrigues, P.F.; Schell, N. Thermomechanical behaviour of shape memory rivet—In situ study, in: ASM International—International Conference on Shape Memory and Superelastic Technologies, SMST 2019 (EID: 2-s2.0-85077261059). 2019. Available online: <https://www.scopus.com/record/display.uri?eid=2-s2.0-85077261059&origin=inward&txGid=8a5b7dd804eee79c6fe2d7ffbeb4f317> (accessed on 6 October 2024).
31. Jape, S.; Young, B.; Haghgouyan, B.; Hayrettin, C.; Baxevanis, T.; Lagoudas, D.C.; Karaman, I. Actuation-Induced stable crack growth in near-equiatomic nickel-titanium shape memory alloys: Experimental and numerical analysis. *Int. J. Solids Struct.* **2021**, *221*, 165–179. [[CrossRef](#)]
32. Exarchos, D.A.; Dalla, P.T.; Tragazikis, I.K.; Dassios, K.G.; Zafeiropoulos, N.E.; Karabela, M.M.; De Crescenzo, C.; Karatza, D.; Musmarra, D.; Chianese, S.; et al. Development and Characterization of High Performance Shape Memory Alloy Coatings for Structural Aerospace Applications. *Materials* **2018**, *11*, 832. [[CrossRef](#)]
33. Ouyang, J.H.; Sasaki, S.; Umeda, K. Low-pressure plasma-sprayed ZrO₂–CaF₂ composite coating for high temperature tribological applications. *Surf. Coat. Technol.* **2001**, *137*, 21–30. [[CrossRef](#)]

Disclaimer/Publisher’s Note: The statements, opinions and data contained in all publications are solely those of the individual author(s) and contributor(s) and not of MDPI and/or the editor(s). MDPI and/or the editor(s) disclaim responsibility for any injury to people or property resulting from any ideas, methods, instructions or products referred to in the content.